AIP Applied Physics Letters

Thermoelectric properties of lattice-matched AlInN alloy grown by metal organic chemical vapor deposition

Hua Tong, Jing Zhang, Guangyu Liu, Juan A. Herbsommer, G. S. Huang et al.

Citation: Appl. Phys. Lett. **97**, 112105 (2010); doi: 10.1063/1.3489086
View online: http://dx.doi.org/10.1063/1.3489086
View Table of Contents: http://apl.aip.org/resource/1/APPLAB/v97/i11
Published by the American Institute of Physics.

Related Articles

Interplay of point defects, biaxial strain, and thermal conductivity in homoepitaxial SrTiO3 thin films
Appl. Phys. Lett. 100, 061904 (2012)

First principles study of Seebeck coefficients of doped semiconductors ZnTe1−xFx and ZnTe1−yNy
J. Appl. Phys. 111, 033701 (2012)

High temperature Seebeck coefficient and resistance measurement system for thermoelectric materials in the thin disk geometry
Rev. Sci. Instrum. 83, 025101 (2012)

High-temperature thermoelectric properties of Cu1–xInTe2 with a chalcopyrite structure
Appl. Phys. Lett. 100, 042108 (2012)

Thermoelectric properties of indium filled and germanium doped Co4Sb12 skutterudites
J. Appl. Phys. 111, 023708 (2012)

Additional information on Appl. Phys. Lett.

Journal Homepage: http://apl.aip.org/
Journal Information: http://apl.aip.org/about/about_the_journal
Top downloads: http://apl.aip.org/features/most_downloaded
Information for Authors: http://apl.aip.org/authors

ADVERTISEMENT

Downloaded 07 Feb 2012 to 128.180.65.141. Redistribution subject to AIP license or copyright; see http://apl.aip.org/about/rights_and_permissions

Thermoelectric properties of lattice-matched AlInN alloy grown by metal organic chemical vapor deposition

Hua Tong,[a] Jing Zhang,[b] Guangyu Liu, Juan A. Herbsommer, G. S. Huang, and Nelson Tansu[c]

Department of Electrical and Computer Engineering, Center for Optical Technologies, Lehigh University, Bethlehem, Pennsylvania 18015, USA

(Received 9 June 2010; accepted 21 August 2010; published online 14 September 2010)

Thermoelectric properties of lattice-matched AlInN grown by metal organic chemical vapor deposition were measured and analyzed. The n-type $Al_{0.83}In_{0.17}N$ alloy exhibited thermal conductivity of 4.87 W/(m K) measured by 3ω differential method. The Seebeck coefficient of n-$Al_{0.83}In_{0.17}N$ was measured as -6.012×10^{-4} V/K by thermal gradient method. The sheet resistivity of n-$Al_{0.83}In_{0.17}N$ was measured by using Van der Pauw method, and the electrical conductivity was measured as $2.38 \times 10^4/(\Omega\ m)$. The thermoelectric figure of merit (Z^*T) of n-type $Al_{0.83}In_{0.17}N$ was measured as 0.532 at room temperature ($T=300$ K). The finding indicates lattice-matched AlInN alloy on GaN as excellent material candidate for thermoelectric application. © *2010 American Institute of Physics*. [doi:10.1063/1.3489086]

III-nitride semiconductors have applications for high power lasers,[1,2] light-emitting diodes for solid state lighting,[3–12] power transistors,[13] and solar cells.[14–17] The requirement of high power density and increasing device integration[1–17] lead to the demand for solid state thermoelectric cooling technology.[18,19] The availability of lattice-matched III-nitride alloy with high thermoelectric figure of merit, which can be integrated with GaN device technology, will have tremendous impact for active thermal cooling of nitride-based high-power devices operating at high-temperature. III-nitride alloys have shown promising results for thermoelectric applications,[20–30] in particular for materials based on GaN,[25–27] InN,[21,22,24] AlGaN,[28] and InGaN[29,30] alloys. However, the studies of AlInN alloy as thermoelectric material have been limited to amorphous material prepared by reactive radio frequency (rf) sputtering.[20–23]

In this work, we present the growths and thermoelectric characterizations of n-type $Al_{0.83}In_{0.17}N$ grown on GaN/sapphire substrate. All samples were grown by metal organic chemical vapor deposition (MOCVD). The thermoelectric properties obtained from the measurements include thermal conductivity (κ), electrical conductivity (σ), Seebeck coefficient (S), and thermoelectric figure of merits (Z^*T).

The growths of the GaN template and AlInN alloys were performed by using vertical-type MOCVD reactor. The group III precursors were TMIn and TMAl. The group V precursor and n-dopant were pure NH_3 and dilute SiH_4, respectively. Purified H_2 was used as carrier gas in the growth of u-GaN, while the growths of AlInN alloy employed N_2 carrier gas. The growths of 2.8 μm u-GaN templates on sapphire were performed by using low temperature GaN buffer, followed by etch-back and recovery process, and then followed by the high temperature growth ($T_g=1080$ °C).

The growths of lattice-matched n-$Al_{0.83}In_{0.17}N$ alloy were carried out at a growth temperature of 780 °C, growth pressure of 20 Torr, rotation speed of 1500 rpm, and V/III molar ratio of 9300. The growth rate of the AlInN material was measured as 2.5 nm/min, and the thickness of the AlInN film is 200 nm. The lattice constant of AlInN epilayer was measured by x-ray diffraction, and the In-content was measured as 17%. The detail of the growths for AlInN by MOCVD is described in Ref. 31.

The thermal conductivity of AlInN film was measured by using the 3ω differential method, which is similar to the approach in Refs. 29, 30, and 35–37. Two samples were prepared for the thermal conductivity measurement as follows: (1) GaN (2.8 μm) grown on sapphire (430 μm) as reference, and (2) n-type $Al_{0.83}In_{0.17}N$ (200 nm) grown on GaN (2.8 μm)/sapphire (430 μm). A 200 nm SiO_2 electrical insulating layer was deposited on these samples by plasma-enhanced chemical vapor deposition, and the metal heater contacts of 20 nm Ti/130 nm Au were deposited by using electron beam evaporator.

Figures 1(a) and 1(b) show the schematic and microscope image, respectively, of the four-probe 3ω measurement set up for the AlInN and GaN samples. In our experiment, a digital lock-in amplifier SR830 was used to supply the driving ac current (I_ω) with sweeping frequency ω and collect the voltage (V_ω) as well as the third harmonic voltage ($V_{3\omega}$) of the metal stripe. A digital multimeter HP 34401A was used to measure the current in order to obtain the metal heater resistance. All measurements were performed at room temperature. The 3ω measurement setup was calibrated by measuring the thermal conductivities of sapphire and SiO_2 using slope[32–34] and differential[35–37] methods. The thermal conductivities of sapphire and SiO_2 ($T=300$ K) were obtained as 41 W/(m K) and 1.1 W/(m K), respectively, in good agreement with reported values.[36,38]

Figure 2 shows the measured voltage V_ω and in-phase $V_{3\omega}$ of (a) the undoped GaN reference sample and (b) the lattice-matched $Al_{0.83}In_{0.17}N$ sample at 300 K. The sweeping frequency of the driving current ($\omega/2\pi$) ranged from 100 to 1000 Hz, which ensured the thermal penetration depth to be larger than the thickness of thin film while smaller than the thickness of the substrate. The temperature oscillation ampli-

[a]Electronic mail: hut3@lehigh.edu.
[b]Electronic mail: jiz209@lehigh.edu.
[c]Electronic mail: tansu@lehigh.edu.

 © 2010 American Institute of Physics

Downloaded 07 Feb 2012 to 128.180.65.141. Redistribution subject to AIP license or copyright; see http://apl.aip.org/about/rights_and_permissions

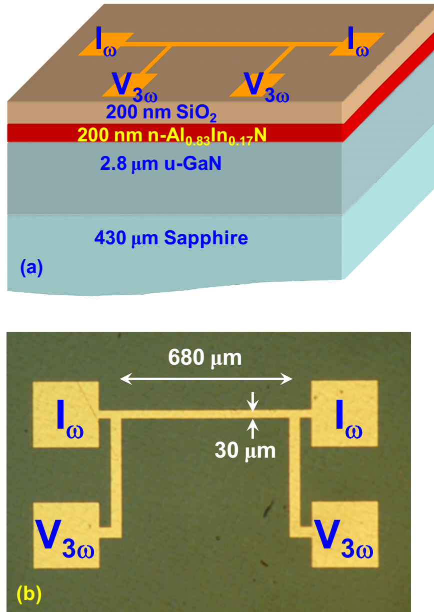

FIG. 1. (Color online) (a) Cross sectional schematic and (b) top microscope image of four-probe 3ω measurement set up for lattice-matched n-$Al_{0.83}In_{0.17}N$ film grown on GaN/sapphire template prepared with SiO_2 insulation layer.

tude of both samples can be obtained from the relation:[32–36]

$$T_{ac} = 2\frac{V_{3\omega}}{V_{\omega}}\frac{dT}{dR}R. \tag{1}$$

Figure 3 shows the temperature oscillation amplitudes T_{ac} as a function of frequency in logarithm scale for both $Al_{0.83}In_{0.17}N$ sample and reference sample. The temperature raise ΔT_{ac} caused by the thin film was calculated by subtracting the T_{ac} of the reference sample from the $Al_{0.83}In_{0.17}N$ sample. The thermal conductivity value of the $Al_{0.83}In_{0.17}N$ thin film layer was obtained as 4.87 W/(m K), which was comparable to AlInN prepared by reactive rf sputtering[20,21] and other nitride-based ternary alloys, such as InGaN (Refs. 29 and 39) and AlGaN.[28,39,40] This finding confirms that alloy scattering in ternary alloy is the dominant factor of phonon scattering that lowers the thermal conductivity significantly from the binary alloys,[39,40] which in turn leads to significant increase in $Z^{*}T$ value for ternary III-Nitride material.[40]

The Hall measurements of the $Al_{0.83}In_{0.17}N$ film were carried out by employing Van der Pauw method, which indicated n-type background carrier density of 5.1×10^{18} cm^{-3} and electron mobility of 290 $cm^{2}/(V\ s)$. The sheet resistivity of lattice-matched $Al_{0.83}In_{0.17}N$ was measured as 210 Ω/sq using Van der Pauw scheme, and its electrical conductivity was measured as $2.38\times10^{4}/(\Omega\ m)$.

The thermal gradient method was used to determine the Seebeck coefficient, similar to the approach in Refs. 29 and 30. When a temperature gradient was created in the sample, as illustrated in Fig. 4(a), both the voltage difference and temperature difference were measured. A hotplate was used to create the high temperature. Two type K thermocouples were attached to the top surface of AlInN via indium (In)

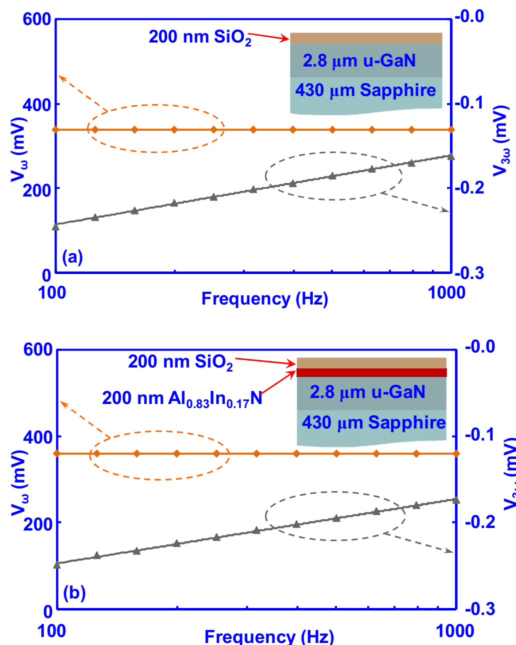

FIG. 2. (Color online) Measured voltage V_{ω} and in-phase $V_{3\omega}$ vs driving frequency from 100 to 1000 Hz for (a) undoped GaN reference sample and (b) lattice-matched n-$Al_{0.83}In_{0.17}N$ sample at 300 K.

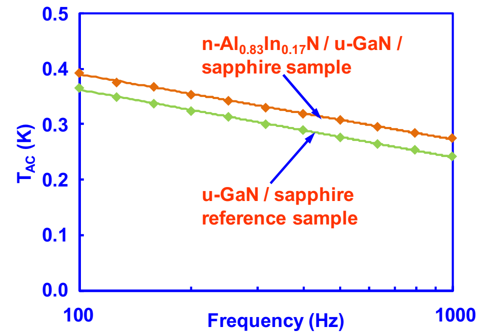

FIG. 3. (Color online) Temperature oscillation amplitude (T_{ac}) as a function of frequency in logarithm scale for n-$Al_{0.83}In_{0.17}N$ sample and GaN/sapphire reference sample.

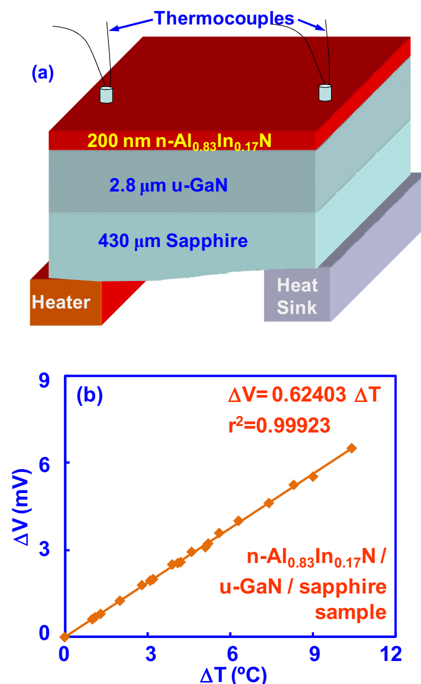

FIG. 4. (Color online) (a) Seebeck measurement schematic for thermal gradient created by heater and heat sink and Seebeck voltage as well as temperature difference measured by two thermocouples, and (b) Seebeck voltage as a function of the temperature difference for $Al_{0.83}In_{0.17}N$ sample measured at room temperature, with linear regression $r^{2}=0.99923$.

Downloaded 07 Feb 2012 to 128.180.65.141. Redistribution subject to AIP license or copyright; see http://apl.aip.org/about/rights_and_permissions

metal to measure temperature difference. The Seebeck voltage was collected from the positive chromel electrodes of the thermocouples at the same time. Figure 4(b) plots the measured Seebeck voltage as a function of the temperature difference. The total Seebeck coefficient of AlInN and chromel electrodes combined was calculated as $-\Delta V/\Delta T$, which was measured as -6.24×10^{-4} V/K. The Seebeck coefficient of chromel at room temperature (21.5 μV/K) (Ref. 41) was compensated to yield the absolute Seebeck coefficient of $Al_{0.83}In_{0.17}N$ as -6.025×10^{-4} V/K.

The power factor $P=S^2\ \sigma$ achieved here was 0.864×10^{-2} W/(m K^2). Then the dimensionless thermoelectric figure of merit $Z^*T=P/\kappa\times T$ of n-$Al_{0.83}In_{0.17}N$ has a value of 0.532 at room temperature (T=300 K). The results showed that the lattice-matched AlInN alloy grown by MOCVD as excellent thermoelectric candidate for efficient thermoelectric power generation and thermal cooling, which can be fully integrated with III-nitride device technology.

In comparison with MOCVD-grown InGaN (Refs. 29 and 30) with similar carrier concentration, the lattice-matched n-AlInN exhibits higher Seebeck coefficient and higher electrical conductivity which results in higher power factor. The higher electrical conductivity for same carrier concentration indicates higher mobility, which is due to the improvement of material quality. The higher Seebeck coefficient suggests larger relaxation time of carriers[39] which is the result of better crystalline quality as well. Even though the lattice-matched AlInN shows increased Seebeck coefficient and electrical conductivity, the thermal conductivity of MOCVD-grown AlInN remains comparable with amorphous AlInN deposited by rf sputtering. The use of crystalline MOCVD-grown AlInN results in higher power factor and low thermal conductivity, which in turn leads to a much higher thermoelectric figure of merit Z^*T of 0.532 at room temperature in comparison to those measured for rf sputtered AlInN (Z^*T=0.005, T=300 K) (Ref. 21) and MOCVD-grown InGaN (Z^*T=0.08, T=300 K).[29] The Z^*T value at room temperature for lattice-matched AlInN was measured as significantly higher than the simulated results reported for AlGaN alloys (Z^*T=0.015, T=300 K).[40]

In summary, the growths and thermoelectric properties of lattice-matched n-$Al_{0.83}In_{0.17}N$ alloy grown by MOCVD are presented. The thermoelectric properties of MOCVD-grown n-$Al_{0.83}In_{0.17}N$ film ($n=5.1\times10^{18}$ cm^{-3}) were measured at room temperature, resulting in thermal conductivity κ of 4.87 W/(m K), electrical conductivity σ of $2.38\times10^4/(\Omega$ m), and absolute Seebeck coefficient S of -6.025×10^{-4} V/K. The power factor (P) for the n-$Al_{0.83}In_{0.17}N$ film was measured as 0.864×10^{-2} W/(m K^2), and the thermoelectric figure of merit Z^*T value of 0.532 was measured at room temperature. This finding indicates the lattice-matched $Al_{0.83}In_{0.17}N$ alloy as excellent thermoelectric material, which can be fully integrated with high-power III-nitride device technologies.

This work is supported by U.S. National Science Foundation (DMR Grant No. 0907260 and ECCS Grant No. 0701421), and Class of 1961 Professorship Funds. Two of the authors (H.T. and J.Z.) contributed equally to this work.

[1]D. Queren, A. Avramescu, G. Bruderl, A. Breidenassel, M. Schillgalies, S. Lutgen, and U. Strauß, Appl. Phys. Lett. **94**, 081119 (2009).
[2]H. Zhao and N. Tansu, J. Appl. Phys. **107**, 113110 (2010).
[3]M. H. Kim, M. F. Schubert, Q. Dai, J. K. Kim, E. F. Schubert, J. Piprek, and Y. Park, Appl. Phys. Lett. **91**, 183507 (2007).
[4]N. F. Gardner, G. O. Muller, Y. C. Shen, G. Chen, S. Watanabe, W. Gotz, and M. R. Krames, Appl. Phys. Lett. **91**, 243506 (2007).
[5]R. A. Arif, Y.-K. Ee, and N. Tansu, Appl. Phys. Lett. **91**, 091110 (2007).
[6]R. A. Arif, H. Zhao, Y.-K. Ee, and N. Tansu, IEEE J. Quantum Electron. **44**, 573 (2008).
[7]H. Zhao, R. A. Arif, and N. Tansu, IEEE J. Sel. Top. Quantum Electron. **15**, 1104 (2009).
[8]H. Zhao, G. Liu, X. H. Li, G. S. Huang, J. D. Poplawsky, S. Tafon Penn, V. Dierolf, and N. Tansu, Appl. Phys. Lett. **95**, 061104 (2009).
[9]K. McGroddy, A. David, E. Matioli, M. Iza, S. Nakamura, S. DenBaars, J. S. Speck, C. Weisbuch, and E. L. Hu, Appl. Phys. Lett. **93**, 103502 (2008).
[10]Y. K. Ee, P. Kumnorkaew, R. A. Arif, J. F. Gilchrist, and N. Tansu, Appl. Phys. Lett. **91**, 221107 (2007).
[11]Y. K. Ee, P. Kumnorkaew, R. A. Arif, H. Tong, H. Zhao, J. F. Gilchrist, and N. Tansu, IEEE J. Sel. Top. Quantum Electron. **15**, 1218 (2009).
[12]Y. K. Ee, P. Kumnorkaew, R. A. Arif, H. Tong, J. F. Gilchrist, and N. Tansu, Opt. Express **17**, 13747 (2009).
[13]U. K. Mishra, P. Parikh, and Y. F. Wu, Proc. IEEE **90**, 1022 (2002).
[14]R. Dahal, B. Pantha, J. Li, J. Y. Lin, and H. X. Jiang, Appl. Phys. Lett. **94**, 063505 (2009).
[15]C. J. Neufeld, N. G. Toledo, S. C. Cruz, M. Iza, S. P. DenBaars, and U. K. Mishra, Appl. Phys. Lett. **93**, 143502 (2008).
[16]M. Jamil, R. A. Arif, Y. K. Ee, H. Tong, J. B. Higgins, and N. Tansu, Phys. Status Solidi A **205**, 1619 (2008).
[17]M. Jamil, H. P. Zhao, J. Higgins, and N. Tansu, Phys. Status Solidi A **205**, 2886 (2008).
[18]G. Chen and A. Shakouri, J. Heat Transfer **124**, 242 (2002).
[19]G. Chen, M. S. Dresselhaus, G. Dresselhaus, J.-P. Fleurial, and T. Caillat, Int. Mater. Rev. **48**, 45 (2003).
[20]S. Yamaguchi, Y. Iwamura, and A. Yamamoto, Appl. Phys. Lett. **82**, 2065 (2003).
[21]S. Yamaguchi, R. Izaki, K. Yamagiwa, K. Taki, Y. Iwamura, and A. Yamamoto, Appl. Phys. Lett. **83**, 5398 (2003).
[22]S. Yamaguchi, R. Izaki, N. Kaiwa, S. Sugimura, and A. Yamamoto, Appl. Phys. Lett. **84**, 5344 (2004).
[23]S. Yamaguchi, R. Izaki, Y. Iwamura, and A. Yamamoto, Phys. Status Solidi A **201**, 225 (2004).
[24]R. Izaki, N. Kaiwa, M. Hoshino, T. Yaginuma, S. Yamaguchi, and A. Yamamoto, Appl. Phys. Lett. **87**, 243508 (2005).
[25]S. Yamaguchi, R. Izaki, N. Kaiwa, and A. Yamamoto, Appl. Phys. Lett. **86**, 252102 (2005).
[26]T. Matsumoto, N. Kaiwa, S. Yamaguchi, A. Yamamoto, M. Funato, and Y. Kawakami, AIP Conf. Proc. **893**, 323 (2007).
[27]A. Sztein, H. Ohta, J. Sonoda, A. Ramu, J. E. Bowers, S. P. DenBaars, and S. Nakamura, Appl. Phys. Express **2**, 111003 (2009).
[28]W. Liu and A. A. Balandin, J. Appl. Phys. **97**, 073710 (2005).
[29]B. N. Pantha, R. Dahal, J. Li, J. Y. Lin, H. X. Jiang, and G. Pomrenke, Appl. Phys. Lett. **92**, 042112 (2008).
[30]B. N. Pantha, R. Dahal, J. Li, J. Y. Lin, H. X. Jiang, and G. Pomrenke, J. Electron. Mater. **38**, 1132 (2009).
[31]G. Y. Liu, H. P. Zhao, J. Zhang, H. Tong, G. S. Huang, and N. Tansu, *Proc. IEEE Photonics Society Annual Meeting 2010* (IEEE, Piscataway, NJ, 2010), paper WY5.
[32]D. G. Cahill and R. O. Pohl, Phys. Rev. B **35**, 4067 (1987).
[33]D. G. Cahill, Rev. Sci. Instrum. **61**, 802 (1990).
[34]D. G. Cahill, Rev. Sci. Instrum. **73**, 3701 (2002).
[35]D. G. Cahill, M. Katiyar, and J. R. Abelson, Phys. Rev. B **50**, 6077 (1994).
[36]S.-M. Lee and D. G. Cahill, J. Appl. Phys. **81**, 2590 (1997).
[37]Z. Bian, M. Zebarjadi, R. Singh, Y. Ezzahri, A. Shakouri, G. Zeng, J.-H. Bahk, J. E. Bowers, J. M. O. Zide, and A. C. Gossard, Phys. Rev. B **76**, 205311 (2007).
[38]F. P. Incropera and D. P. De Witt, *Fundamentals of Heat and Mass Transfer*, 5th ed. (Wiley, New York, 2001).
[39]H. Tong, H. P. Zhao, V. A. Handara, J. A. Herbsommer, and N. Tansu, Proc. SPIE **7211**, 721103 (2009).
[40]W. Liu and A. A. Balandin, J. Appl. Phys. **97**, 123705 (2005).
[41]W. Gee and M. Green, J. Phys. E **3**, 135 (1970).

Downloaded 07 Feb 2012 to 128.180.65.141. Redistribution subject to AIP license or copyright; see http://apl.aip.org/about/rights_and_permissions